JAERI 1286

JAERI 1286

Experimental Study on Neutron Dosimeters with Low Threshold Energies

August 1983

日 本 原 子 力 研 究 所

Japan Atomic Energy Research Institute

JAERI レポートは，日本原子力研究所が研究成果編集委員会の審査を経て不定期に公刊している研究報告書です。

入手の問合わせは，日本原子力研究所技術情報部情報資料課（〒319-11茨城県那珂郡東海村）あて，お申しこしください。なお，このほかに財団法人原子力弘済会資料センター（〒319-11 茨城県那珂郡東海村日本原子力研究所内）で複写による実費頒布をおこなっております。

JAERI reports are reviewed by the Board of Editors and issued irregularly.

Inquiries about availability of the reports should be addressed to Information Section, Division of Technical Information, Japan Atomic Energy Research Institute, Tokai-mura, Naka-gun, Ibaraki-ken 319-11, Japan.

編集兼発行　日本原子力研究所
印　　刷　いばらき印刷㈱

Experimental Study on Neutron Dosimeters with Low Threshold Energies

Kiyoshi SAKURAI

Department of JMTR Projects,
Oarai Research Establishment,
Japan Atomic Energy Research Institute
Oarai-machi, Higashiibaraki-gun, Ibaraki-ken, Japan

Received January 7, 1983

Abstract

An important point requiring consideration in studying radiation damage for reactor materials is neutron dosimetry with 0.1～1 MeV range. There are only a few dosimeters sensitive to neutron with energy from 0.1 to 1 MeV for thermal neutron reactor, and the practical use is currently made only of those based on the dosimeters ^{103}Rh(n,n')^{103m}Rh and ^{237}Np(n,f)FP. New dosimeters ^{199}Hg(n,n')^{199m}Hg, ^{93}Nb(n,n')^{93m}Nb and ^{107}Ag(n,n')^{107m}Ag were studied to measure neutron with energy from 0.1 to 1 MeV. This paper describes the neutron cross section measurement for the ^{199}Hg(n,n')^{199m}Hg reaction from 0.78 to 6.3 MeV and the use of cross section data for neutron spectrum unfolding, measurement of neutron fluence above 0.1 MeV with the dosimeter ^{93}Nb(n,n')^{93m}Nb, and use of new dosimeter ^{107}Ag(n,n')^{107m}Ag for neutron spectrum unfolding.

The fission spectrum averaged cross section for the ^{199}Hg(n,n')^{199m}Hg reaction was calculated by using the Watt-type fission spectrum, and was compared with the measured one. The calculated one is about 5% smaller than the measured one. The total neutron flux calculated from the unfolded neutron spectrum with ^{199}Hg(n,n')^{199m}Hg reaction rate was 1% smaller than that without the reaction rate. The uncertainty of the neutron fluence above 0.1 MeV measured with the dosimeter ^{93}Nb(n,n')^{93m}Nb is smaller than ±30%, including the uncertainties of the half-life, the branching ratio, the ^{93}Nb(n,n')^{93m}Nb cross section, and the neutron spectrum. The calculated reaction rate for ^{107}Ag(n,n')^{107m}Ag reaction was 12.8% smaller than that of measured reaction rate.

Keywords: Reactor Materials, Radiation Damage, 0.1～1 MeV, Neutron Dosimetry, Low Threshold Energies, ^{199}Hg(n,n')^{199m}Hg, ^{93}Nb(n,n')^{93m}Nb, ^{107}Ag(n,n')^{107m}Ag, Neutron Cross Section, Neutron Spectrum, Unfolding, Neutron Fluence

低しきい値中性子ドシメータに関する実験的研究

日本原子力研究所大洗研究所材料試験炉部

桜井　淳

1983年1月7日受理

要旨

原子炉材料の照射損傷を究明する上で0.1～1 MeV領域の中性子線量評価が重要になってきている．このエネルギーの中性子に感度をもつ中性子ドシメータは，熱中性子炉に対してわずかしかなく，現在実用化されているものは^{103}Rh$(n,n')^{103m}$Rhおよび^{237}Np(n,f)FPのみである．このエネルギーをカバーする新しい中性子ドシメータ^{199}Hg$(n,n')^{199m}$Hg，^{93}Nb$(n,n')^{93m}$Nbおよび^{107}Ag$(n,n')^{107m}$Agの実用化研究を行った．この論文は，^{199}Hg$(n,n')^{199m}$Hg反応の中性子断面積測定およびその反応を利用した中性子スペクトル・アンホールディングの試み，^{93}Nb$(n,n')^{93m}$Nbによる0.1 MeV以上の中性子フルエンスの測定，^{107}Ag$(n,n')^{107m}$Agによる中性子スペクトル・アンホールディングの試みについてまとめたものである．

測定した中性子断面積とWatt型核分裂スペクトルから核分裂スペクトル平均断面積を計算し，実測値と比較した．その結果，計算値が実測値よりも約5％小さいことがわかった．ドシメータ^{199}Hg$(n,n')^{199m}$Hgを含む10種類のドシメータを利用して弥生炉グローリホールの中性子スペクトル・アンホールディングを試みた．ドシメータ^{199}Hg$(n,n')^{199m}$Hgを利用した場合，全中性子束の変化はわずか1％であった．ドシメータ^{93}Nb$(n,n')^{93m}$Nbで測定した0.1 MeV以上の中性子フルエンスの不確定は，利用した核データおよび中性子スペクトルの不確定を考慮しても，±30％以下であった．^{107}Ag$(n,n')^{107m}$Ag反応の計算反応率は，実測値よりも12.8％小さい．この原因は，中性子断面積を過小評価したためである．

Contents

目　　次

1. Introduction

Neutron was discovered by J. Chadwick in 1932. Activation reaction induced by neutron was discovered by E. Fermi in 1934. Since then, the activation reaction has been used in the fields of nuclear physics, reactor physics, reactor neutron dosimetry and so on.

Many foils, being activated by neutrons with reactions such as (n,γ), (n,p), (n,α) and $(n,2n)$ reactions, have been used as neutron dosimeters[1-4] for measuring the neutron flux and the neutron spectrum in a reactor core. The foil activation method is very important in the field of reactor neutron dosimetry[1-4]. The advantages of the activation are as follows: (1) the influence to neutron field is very little because of the small foil, (2) the activation induced by gamma-rays in reactor core is negligibly small, (3) it is applicable to the neutron field with low and high neutron flux, (4) the foil with high purity and low cost is available, and (5) it is easy to measure the activity. The disadvantage is as follows: (1) the accuracy and the precision of the result depend on those of the nuclear data such as neutron cross section data. Therefore accurate and precise neutron cross section data are very important.

The neutron dosimeters used at present are shown in **Fig. 1.1**[5]. The half-life and the sensitive energy range of each dosimeter are shown in **Fig. 1.1**. The sensitive energy range shown with solid line is for thermal neutron reactor, and the range shown with dashed line is for fast neutron reactor. The feasibility of the dosimeter $^{93}Nb(n,n')^{93m}Nb^{\dagger}$ is under study.

There are only a few dosimeters sensitive to neutron with energy from 0.1 to 1 MeV for

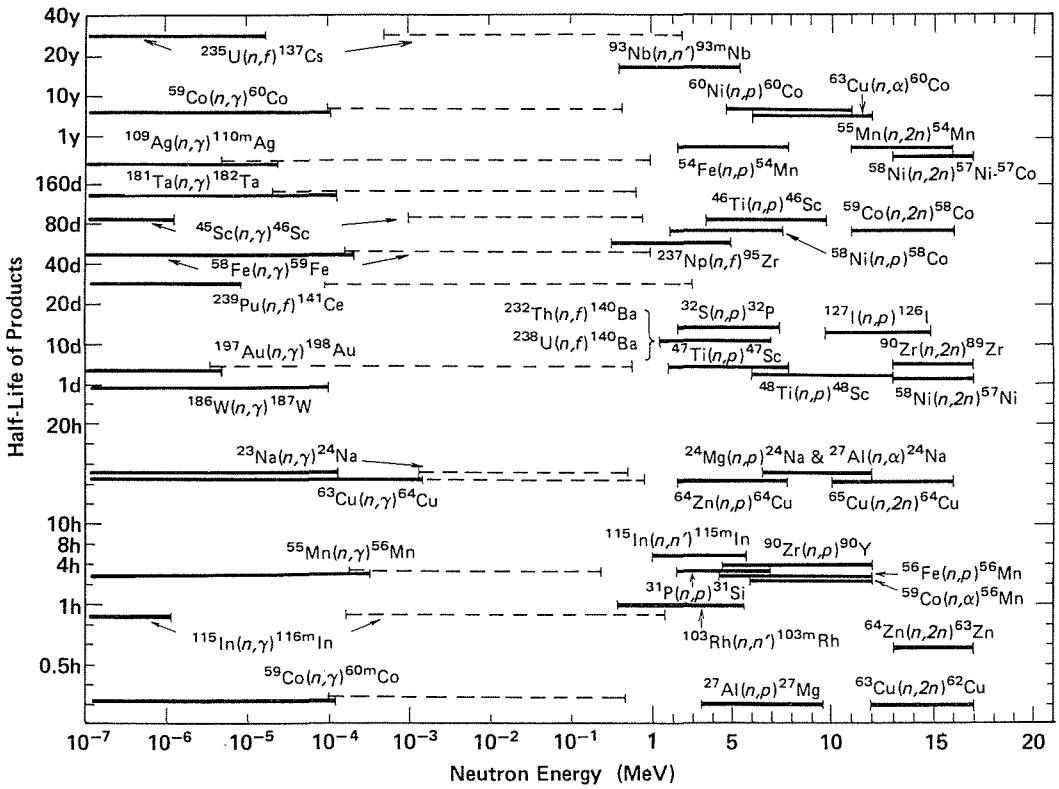

Solid line is for thermal neutron reactor, and dashed line, for fast neutron reactor.

Fig. 1.1 Half-life and sensitive energy range of neutron dosimeter[5].

† Dosimeter $^{93}Nb(n,n')^{93m}Nb$ means neutron dosimeter with $^{93}Nb(n,n')^{93m}Nb$ reaction.

thermal neutron reactor, and the practical use is currently made only of those based on the dosimeters ^{103}Rh(n,n')^{103m}Rh and ^{237}Np(n,f)FP. The author has been studying new dosimeters sensitive to neutron with energy from 0.1 to 1 MeV. The dosimeters are ^{199}Hg(n,n')^{199m}Hg, ^{93}Nb(n,n')^{93m}Nb and ^{107}Ag(n,n')^{107m}Ag. The threshold energies are about 0.5, 0.1 and 0.1 MeV for ^{199}Hg(n,n')^{199m}Hg, ^{93}Nb(n,n')^{93m}Nb and ^{107}Ag(n,n')^{107m}Ag reactions, respectively.

Because of its low threshold energy of about 532 keV, the ^{199}Hg(n,n')^{199m}Hg reaction is important as a neutron dosimeter, especially for a nuclear reactor[6]. The isomeric state at 532 keV of ^{199}Hg decays with a half-life of 42.6 minutes and can be produced by neutron inelastic scattering by either direct excitation or more probably through excitation to higher levels followed by deexcitation to this isomeric state[7]. This does not decay directly to the ground state, but is deexcited by a 374 keV M4 transition in cascade with a 158 keV E2 transition[7]. The cross sections for the ^{199}Hg(n,n')^{199m}Hg reaction have been poorly known; especially the cross section data above 3 MeV have not been found except at 14.4 MeV. Swann and Metzger[8] measured the cross sections from threshold energy to 2.2 MeV about 25 years ago. Bornemisza et al.[9] measured the cross section at 2.8 MeV, and Temperly[10] and Hankla et al.[11] measured it at 14.4 MeV. Cross sections from threshold energy to about 6 MeV for the ^{199}Hg(n,n')^{199m}Hg reaction are required in order to use the reaction for the reactor neutron dosimetry. Evaluated neutron cross sections for the activation and/or fission reactions are available, for example the ENDF Dosimetry File is often used for neutron dosimetry. But the evaluated neutron cross sections for the ^{199}Hg(n,n')^{199m}Hg reaction were not available. Therefore the author measured cross sections from 0.78 to 6.3 MeV using a 5.5 MV Van de Graaff accelerator at the Japan Atomic Energy Research Institute. In this paper the author has tried to apply the result of the dosimeter to an unfolding procedure.

The dosimeter ^{93}Nb(n,n')^{93m}Nb has some advantages for monitoring neutron fluence above 0.1 MeV. These advantages are as follows:

1. The threshold energy is as low as ~30 keV[7].
2. The half-life is as long as 13.6 years[7].
3. The excitation function is similar to the shape of damage function.

Therefore, the dosimeter has been tried to monitor neutron fluence above 0.1 MeV in the light water reactor pressure vessel[12]. Neutron fluence above 0.1 MeV was measured with the dosimeter at the second beryllium reflector region in the Japan Materials Testing Reactor (JMTR). The neutron fluence was compared with that monitored with the dosimeter ^{54}Fe(n,p)^{54}Mn.

Among the different types of dosimeters that mignt be utilized for neutron spectrum measurements from 0.1 to 1 MeV, the practical use is only the dosimeters ^{103}Rh(n,n')^{103m}Rh, besides fission foils such as Np. For this reason, rhodium has been extensively studied in respect to cross section and decay data[13-15]. Now, effective threshold energies lower than Rh are presented by dosimeters ^{107}Ag(n,n')^{107m}Ag and ^{109}Ag(n,n')^{109m}Ag. Hence, Ag-foil might serve as usefully as Rh in neutron dosimetry for covering this energy region below 1 MeV. The author has performed an experimental study using the YAYOI, a fast neutron source reactor, to verify the possibilities of utilizing Ag-foil in reactor neutron dosimetry.

This paper consists of five chapters: 1. Introduction, 2. Cross Section Measurement for the ^{199}Hg(n,n')^{199m}Hg Reaction from 0.78 to 6.3 MeV†, and the Use of Cross Section Data for Neutron Spectrum Unfolding, 3. Measurement of Neutron Fluence above 0.1 MeV with the Dosimeter ^{93}Nb(n,n')^{93m}Nb, 4. Use of New Dosimeter ^{107}Ag(n,n')^{107m}Ag for Neutron Spectrum Unfolding, 5. Conclusion.

---

† J. Nucl. Sci: Technol., **19**, 775 (1982).

2. Cross Section Measurement for the $^{199}Hg(n,n')$ ^{199m}Hg Reaction from 0.78 to 6.3 MeV, and the Use of Cross Section Data for Neutron Spectrum Unfolding

2.1 Cross Section Measurement for the $^{199}Hg(n,n')^{199m}Hg$ Reaction from 0.78 to 6.3 MeV

2.1.1 Experimental Method

2.1.1.1 Irradiation

An experimental arrangement for the measurement of the cross section for the $^{199}Hg(n,n')$ ^{199m}Hg reaction is shown in **Fig. 2.1**. Monoenergetic neutrons were produced by the $D(d,n)^3He$ and $^7Li(p,n)^7Be$ reactions. The neutron energy was changed by varying the projectile energy and the angle (0°, 90°, 120° and 150°).

A lithium target was prepared by the vacuum evaporation of natural lithium fluoride (LiF) onto a titanium backing foil. The thickness of the lithium fluoride layer is about 500 $\mu g/cm^2$ which corresponds to an energy loss of about 60 keV for 2 MeV protons. A deuterium target supplied by the Radiochemical Center was used. By cooling the target with a jet of air, no appreciable decrease in neutron yield was observed for 20 hours with a beam current up to about 2 μA in a 20 mm^2 spot.

Mercury samples were fabricated by pressing mercury sulphate (Hg_2SO_4) powder into a form of disk with 20 mm in diameter and about 3 mm in thickness. The density of the sample resulted in about 5.3 g/cm^3. Each of the sample was sandwiched by indium foils of the same diameter and 0.5 mm in thickness. The distance between the neutron target and the sample was about 3 cm.

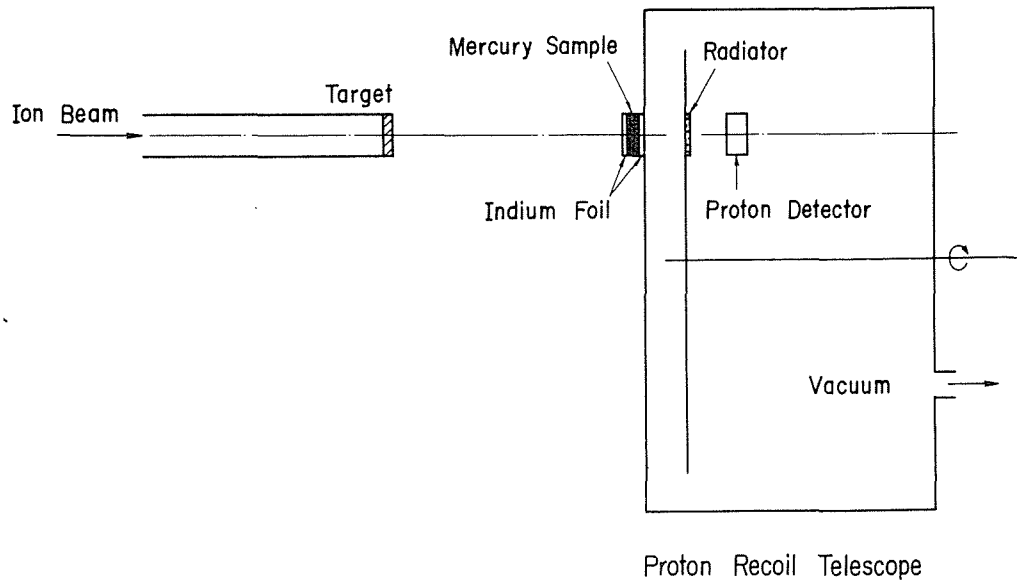

Fig. 2.1 Experimental arrangement for the measurement of the cross section for the $^{199}Hg(n,n')^{199m}Hg$ reaction.

2.1.1.2 Neutron flux† determination

A proton recoil telescope counter and indium foils were used to determine the absolute neutron flux for the measurement of the cross section for the $^{199}Hg(n,n')^{199m}Hg$ reaction. Neutron flux determination by the indium foils was based on the $^{115}In(n,n')^{115m}In$ reaction. The cross sections for this reaction were taken from ENDF/B-V Dosimetry File[16]. A proton recoil telescope counter consisted of a polyethylene radiator and a proton detector. The author used a silicon surface barrier detector for neutron energy below 5 MeV[17], while above 5 MeV the author used a CsI(Tl) detector[18], because the Si(n,p) and (n,α) reactions produced by neutrons above 5 MeV become error factor for the measurement of recoiled proton[19].

The polyethylene radiator and the proton detector were set in a vacuum chamber as shown in **Fig. 2.1**. The polyethylene radiator was fixed on a rotary disk in the chamber, and it was put in and out in front of the proton detector to distinguish recoiled protons from the radiator or those from other materials. A mercury sample sandwiched by the indium foils was fixed on the surface of the chamber.

The neutron detection efficiency of the proton recoil telescope counter was calculated by the method which had been proposed by Gotoh and Yagi[20]. The accuracy of the H(n,n) cross section is about 1% up to 8 MeV[21,22]. The uncertainty of the neutron detection effi ciency was about 3%.

2.1.1.3 Activity measurement

Neutron irradiation was usually performed for one or two hours. After the irradiation, the gamma activities of the mercury samples and the indium foils were measured with a high purity germanium detector for more than one hour. The germanium detector was a vertical mount single end type with 42.5 mm in diameter and 59.9 mm in length. Each sample was put on the surface of the Ge detector.

The detection efficiency of gamma-rays was determined by using gamma-ray standard sources such as ^{152}Eu, ^{57}Co, ^{137}Cs, ^{54}Mn and ^{60}Co of which each activity was about 0.1 μCi. The efficiencies not only at the central point on the detector surface but also at 10 points were determined in the range of ±10 mm horizontally on the detector surface, because the diameter of present samples were 20 mm. The efficiencies at 1, 2 and 3 mm in height were also measured in the same way. The difference of the efficiency is about 5% for horizontal surface and also each vertical position.

The half-lives of ^{199m}Hg and ^{115m}In are 42.6 ± 0.2 minutes and 4.486 ± 0.004 hours, respectively[7]. The branching ratios are 52.3 ± 0.5 % and 12.3 ± 0.5 % for the 158 keV and 374 keV gamma-rays of ^{199m}Hg, and 45.9 ± 0.1 % for the 336 keV gamma-ray of ^{115m}In, respectively[7]. All other nuclear decay data for the standard sources were also cited from Ref. 7.

The self-absorption of the gamma-rays in the mercury sample was theoretically calculated by the Monte Carlo method[23]. The result showed that the self-absorptions for the 158 keV and 374 keV gamma-rays were about 80.0 ± 2.4 % and 32.4 ± 1.3 %, respectively. The self-absorption of the 336 keV gamma-ray in the indium foil was less than 1%.

2.1.2 Results

The neutron cross section is calculated from the activity data and the determined neutron flux:

$$A=\frac{\lambda N}{1-e^{-\lambda t_c}}\frac{1}{I}\frac{1}{\eta}e^{\lambda t_w} \qquad (2.1)$$

† Neutron flux means neutron flux density (n/cm^2·sec) in this paper.

where A : activity (dps)
λ : decay constant (sec^{-1})
N : KX-ray or gamma-ray peak area
I : branching ratio
η : detection efficiency
t_c : counting time (sec)
t_w : waiting time from irradiation end to counting start (sec)

$$R=\frac{A}{N_o\frac{am}{M}(1-e^{-\lambda t_{ir}})} \tag{2.2}$$

where R : Neutron reaction rate (dps/atom)
N_o : Avogadro number (6.022×10^{23} $mole^{-1}$)
M : atomic weight (amu)
a : abundance
m : sample weight (g)
t_{ir} : irradiation time (sec)

$$\sigma(E)=\frac{\text{neutron reaction rate}}{\text{neutron flux}}=\frac{R}{\phi(E)} \tag{2.3}$$

where $\sigma(E)$: neutron cross section (cm^2)
$\phi(E)$: neutron flux ($n/cm^2 \cdot sec$)

When the neutron flux is determined with indium foil, the neutron cross section is expressed as follows:

$$\sigma(E)=\frac{R}{R'}\sigma'(E) \tag{2.4}$$

where R : $^{199}Hg(n,n')^{199m}Hg$ reaction rate
R' : $^{115}In(n,n')^{115m}In$ reaction rate
$\sigma'(E)$: $^{115}In(n,n')^{115m}In$ cross section

The cross sections measured for the $^{199}Hg(n,n')^{199m}Hg$ reaction are given in **Table 2.1**. The present results of the cross sections for the reaction are also shwon in **Fig. 2.2** compared with the previous data[8-11]. The previous data are also plotted in **Fig. 2.2**. The errors estimated in the present measurement are given in **Table 2.2**. The cross sections at neutron energies of 1.79, 2.27, 3.07 and 3.25 MeV were determined by neutron flux measurement with the indium foils. The errors of these cross sections are larger than those of other cross sections, because the samples were irradiated at the angles shown in **Table 2.1** and each activity was very weak. The errors are about 13, 16, 15 and 13% for the neutron energies of 1.79, 2.27, 3.07 and 3.25 MeV, respectively. The errors of the cross sections at the neutron energies except neutron energies of 1.79, 2.27, 3.07 and 3.25 MeV are about from 11 to 12%. The cross sections at neutron energies of 0.78, 1.20, 1.82 and 4.92 MeV were determined by neutron flux measurement with the proton recoil telescope counter and the indium foils. Good agreement can be seen in those cross sections except the one at the neutron energy of 0.78 MeV. For the neutron energy of 0.78 MeV, the cross section determined by neutron flux measurement made with the indium foils is more reliable than that determined by neutron flux measurement with the proton recoil telescope counter, because the counting number of the recoiled proton was not enough.

The errors of neutron energies are attributed to the energy spread derived from the angles subtended by the mercury sample. The main errors are attributed to counting of gamma-rays emitted from ^{199m}Hg and ^{115m}In for the neutron flux measurement with the

Table 2.1 Obtained cross sections for the $^{199}Hg(n,n')^{199m}Hg$ reaction from 0.78 to 6.3 MeV

Neutron energy (MeV)	Neutron source	Cross section by In monitoring		Cross section by recoil proton monitoring	
		^{199m}Hg; 158 keV	^{199m}Hg; 374 keV	^{199m}Hg; 158 keV	^{199m}Hg; 374 keV
0.784 ± 0.031	Li(p,n) $\theta = 0°$	33.8 ± 3.7 mb	31.0 ± 3.6 mb	59.9 ± 4.2 mb	52.3 ± 4.2 mb
0.994 ± 0.039	Li(p,n) $\theta = 0°$			77.7 ± 4.9	73.0 ± 5.2
1.20 ± 0.040	Li(p,n) $\theta = 0°$	96.3 ± 10.6	90.9 ± 10.0	105 ± 6	99.6 ± 5.6
1.79 $\pm^{0.147}_{0.097}$	D(d,n) $\theta = 150°$	201 ± 26	206 ± 31		
1.82 ± 0.050	Li(p,n) $\theta = 0°$	242 ± 27	225 ± 24	270 ± 14	250 ± 14
2.27 $\pm^{0.295}_{0.231}$	D(d,n) $\theta = 120°$	327 ± 51			
3.07 $\pm^{0.410}_{0.361}$	D(d,n) $\theta = 90°$	413 ± 61	489 ± 92		
3.25 $\pm^{0.360}_{0.324}$	D(d,n) $\theta = 90°$	412 ± 53	403 ± 66		
4.92 ± 0.095	D(d,n) $\theta = 0°$	650 ± 72	600 ± 70	662 ± 36	611 ± 39
6.27 ± 0.065	D(d,n) $\theta = 0°$	653 ± 72	686 ± 80		

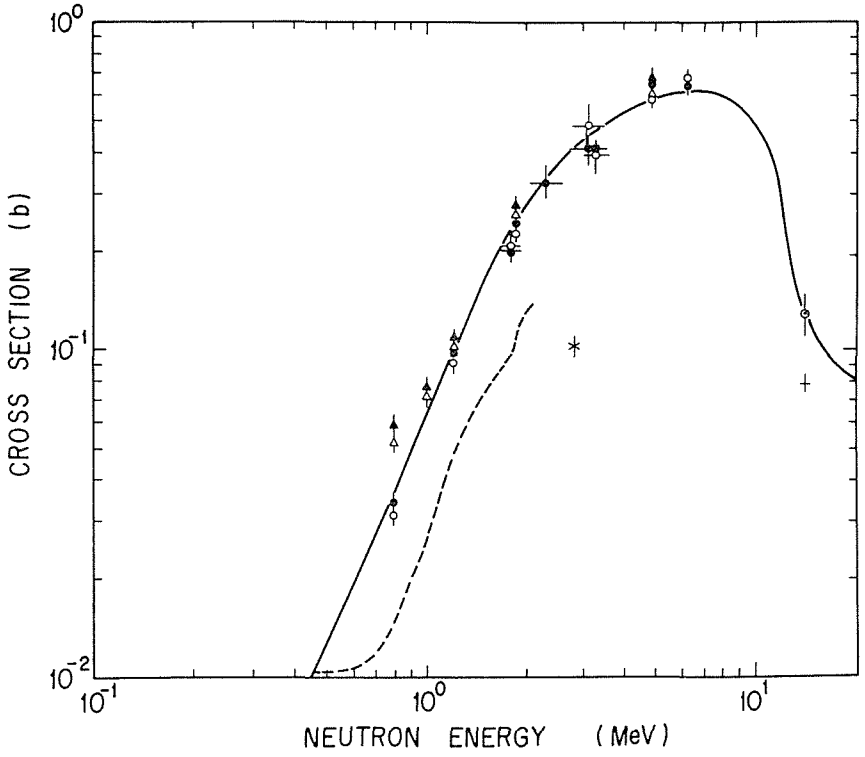

Present works

● Indium monitor, ^{199m}Hg 158 keV — Fitting curve --- Swan and Metzger[8)]
○ " " 374 keV × Bornemisza et al.[9)]
▲ Proton recoil counter, 158 keV ⊙ Hankla et al.[11)]
△ " " 374 keV + Temperley[10)]

Fig. 2.2 Cross section for the $^{199}Hg(n,n')^{199m}Hg$ reaction.

Table 2.2 Summary of the estimated errors in the cross section measurement

(1) For the indium neutron flux monitoring		
$^{115}In(n,n')^{115m}In$ cross section (ENDF/B-V covariance file)		10 %
Ge detector efficiency		3 %
^{199m}Hg 158 and 374 keV gamma-ray measurement		2.1 – 14.3 %
^{115m}In 336 keV gamma-ray measurement		0.6 – 6.2 %
Others		2 %
	Total	10.9 – 18.9 %
(2) For the proton neutron flux monitoring		
Proton recoil telescope counter efficiency		3 %
Recoil proton counting		2.0 – 4.8 %
Ge detector efficiency		3%
^{199m}Hg 158 and 374 keV gamma-ray measurement		1.5 – 4.3 %
Others		2 %
	Total	5.3 – 8.0 %

indium foils, and counting of gamma-rays emitted from ^{199m}Hg and recoiled proton for the neutron flux measurement with the proton recoil telescope counter. Each error was added quadratically yielding of 11 to 19% for the indium neutron flux monitoring and from 5 to 8% for the proton recoil neutron flux monitoring.

2.1.3 Discussion

A comparison of the present data with others is limited to two sets of data: the cross sections measured by Swann and Metzger[8] are generally 50% lower then the present data. The cross section at the neutron energy of 2.8 MeV measured by Bornemisza et al.[9] is about 75% lower than the present data.

For the use of the present data in the neutron dosimetry experiment, the present data and Hankla's data[11] were fitted with an impirical formula shown by Cross and Ing[24] . The cross sections for the neutron energy of 0.78 MeV determined by neutron flux measurement made with the indium foils were used for the fitting. The fitting formula is the following,

$$\sigma(E) = 0.082 - \frac{0.67}{1+\left(\frac{E}{2.32}\right)^{2.66}} + \frac{0.588}{1+\left(\frac{E}{11.44}\right)^{10}} \tag{2.5}$$

where $\sigma(E)$ is neutron cross section in barn and E is neutron energy in MeV.

The fission spectrum averaged cross section is defined by the following equation:

$$\bar{\sigma} = \frac{\int_0^\infty \phi(E)\sigma(E)dE}{\int_0^\infty \phi(E)dE} \tag{2.6}$$

where $\phi(E)$: fission spectrum

$\sigma(E)$: neutron cross section

In this calculation, the Watt-type fission spectrum[25] was used. The spectrum is expressed as follows:

$$\phi(E)=e^{-E/a}\sinh\sqrt{bE} \tag{2.7}$$

$$\bar{E}=3a/2+ba^2/4$$

$$a=0.998\ \text{MeV}$$

$$b=2.249\ \text{MeV}^{-1}$$

where E : neutron energy (MeV)

The fission spectrum averaged cross section was calculated by using the formula, and was compared with the measured one. The calculated one is 238.3 mb for the Watt-type fission spectrum. The measured one is 252.3 mb[26]. The calculated one for the Watt-type fission spectrum is about 5% smaller than the measured one.

2.2 Use of New Dosimeter ^{199}Hg(n,n')^{199m}Hg for Neutron Spectrum Unfolding

2.2.1 Nuclear Data for the ^{199}Hg(n,n')^{199m}Hg Reaction

2.2.1.1 Abundance

The author has used natural mercury sample (HgO), because enriched ^{199}Hg sample is very expensive (about 100$/1mg). The mercury element consists of seven isotopes. Each abundance is as follows[27]; ^{196}Hg(0.15%), ^{198}Hg(10.1%), ^{199}Hg(16.9%), ^{200}Hg(23.1%), ^{201}Hg (13.2%), ^{202}Hg(29.7%) and ^{204}Hg(6.8%).

2.2.1.2 Half-life and gamma-branching ratio of ^{199m}Hg

The excited state of ^{199}Hg is shown in **Fig. 2.3**[7]. The threshold energy of the ^{199}Hg(n,n')^{199m}Hg reaction is about 532 keV, the isomer half-life is 42.6 ± 0.2 minutes and the multipolarity of the transition from the isomeric state to the 158 keV level is M4 and that from 158 keV level to the ground state is E2[7]. The branching ratios are 52.3 ± 0.5 % and 12.3 ± 0.5 % for the 158 and 374 keV gamma-rays, respectively[7].

2.2.1.3 Cross sections for the ^{199}Hg(n,n')^{199m}Hg reaction

Energy dependent cross sections for the ^{199}Hg(n,n')^{199m}Hg reaction was not available[6]. Swann and Metzger[8] measured the cross sections from the threshold energy to 2.2 MeV. Bornemisza et al.[9] measured the cross section at 2.8 MeV. Hankla et al.[11] measured the cross section at 14.4 MeV. From these data, it is impossible to evaluate a reliable neutron cross section for neutron spectrum unfolding. Therefore, the author measured the cross sections from 0.78 to 6.3 MeV. The neutron cross section for neutron spectrum unfolding was evaluated from the data measured by the author and by Hankla et al.[11].

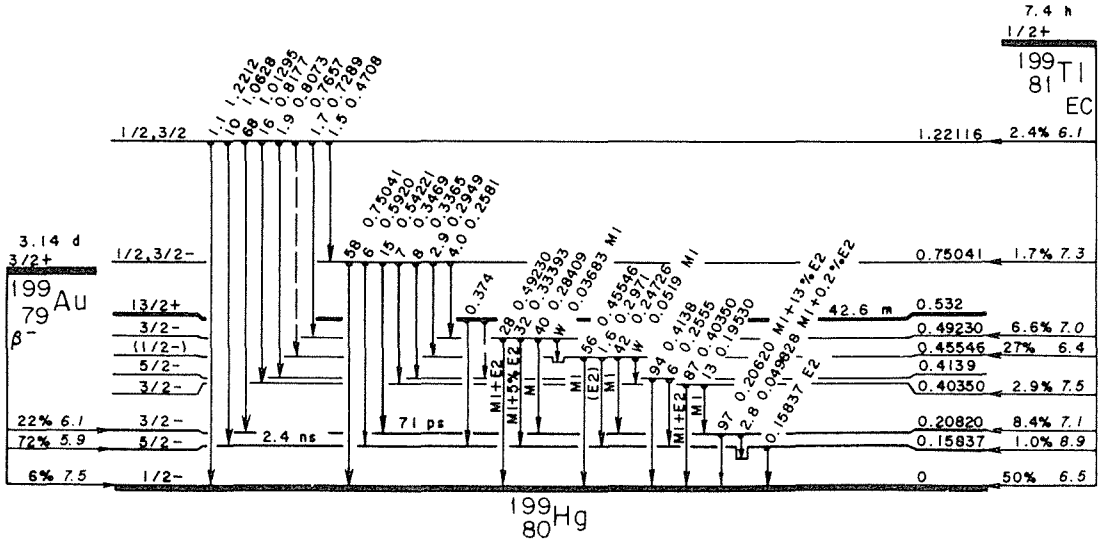

Fig. 2.3 Excited state of ^{199}Hg[7].

2.2.2 Reaction-rate Measurement and Neutron Spectrum Unfolding

The validity of the dosimeter $^{199}Hg(n,n')^{199m}Hg$ for reactor neutron dosimetry has been examined through an irradiation experiment using the standard neutron field (glory-hole) in the YAYOI. The neutron spectrum had been accurately evaluated by repeated measurements and by calculation[28].

The irradiation of foils in the YAYOI glory-hole was performed at a reactor power of 500 W and an irradiation time of 30 minutes. The measured reaction rates of the $^{199}Hg(n,n')^{199m}Hg$, $^{27}Al(n,\alpha)^{24}Na$, $^{24}Mg(n,p)^{24}Na$ and $^{115}In(n,n')^{115m}In$ reactions are given in **Table 2.3**[26]. The reaction rates of the $^{59}Co(n,\alpha)^{56}Mn$, $^{56}Fe(n,p)^{56}Mn$, $^{27}Al(n,p)^{27}Mg$, $^{27}Al(n,\alpha)^{24}Na$, $^{24}Mg(n,p)^{24}Na$, $^{23}Na(n,\gamma)^{24}Na$, $^{47}Ti(n,p)^{47}Sc$, $^{48}Ti(n,p)^{48}Sc$ and $^{115}In(n,n')^{115m}In$ reactions measured by dosimetry group at the University of Tokyo are also given in **Table 2.3**[29]. The gamma-ray spectrum of ^{199m}Hg is shown in **Fig. 2.4**.

Table 2.3 Experimental reaction rate[29] and neutron cross sections

Reaction	YAYOI glory-hold reaction rate (dps/atom) (reactor power 500 W)		Neutron cross section for unfolding
	Sakurai's data set[29]	The University of Tokyo dosimetry group[29]	
$^{199}Hg(n,n')^{199m}Hg$	2.89−14+(±4%)		chap. 2, 2.1
$^{59}Co(n,\alpha)^{56}Mn$		1.47−17 (±2.4%)	ENDF/B-V
$^{56}Fe(n,p)^{56}Mn$		1.00−16 (±2.8%)	"
$^{27}Al(n,p)^{27}Mg$		3.87−16 (±8.4%)	"
$^{27}Al(n,\alpha)^{24}Na$	6.91−17 (±3%)	6.74−17 (±2.9%)	"
$^{24}Mg(n,p)^{24}Na$	1.40−16 (±3%)	1.47−16 (±3.1%)	"
$^{23}Na(n,\gamma)^{24}Na$		7.85−17 (±4.1%)	"
$^{47}Ti(n,p)^{47}Sc$		1.68−17 (±11.5%)	"
$^{48}Ti(n,p)^{48}Sc$		2.57−17 (±3.8%)	"
$^{115}In(n,n')^{115m}In$	2.14−14 (±3%)	2.12−14 (±3.9%)	"

+ 2.89−14 means 2.89×10^{-14}

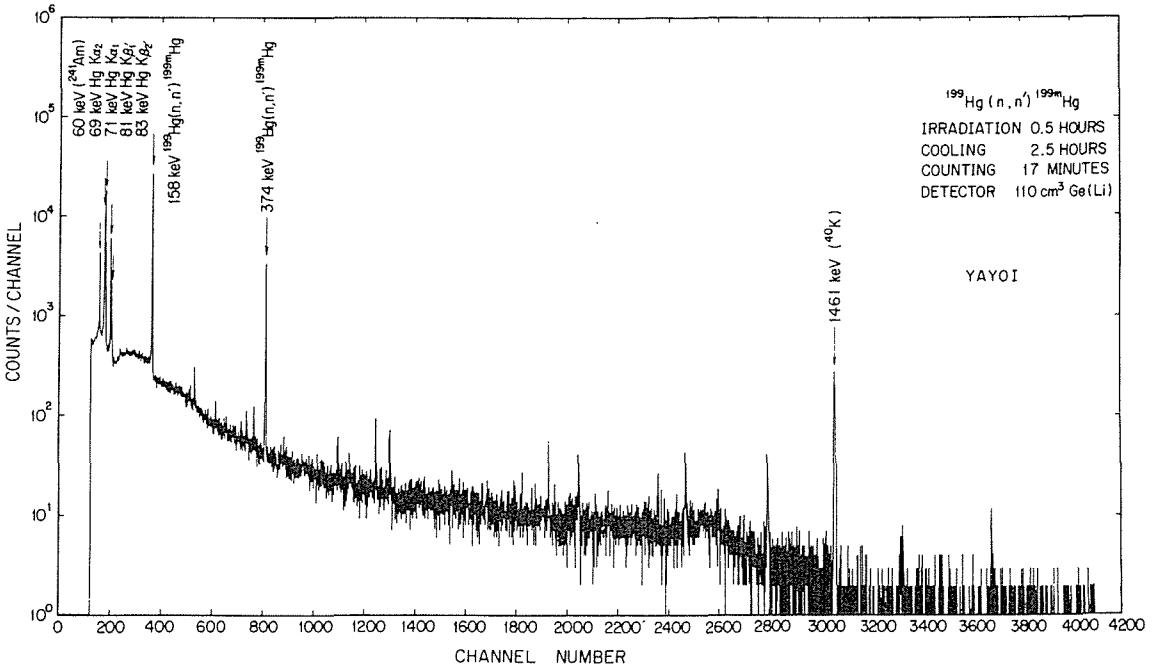

Fig. 2.4 Gamma-ray spectrum of ^{199m}Hg.

The code SAND II[30] was used for neutron spectrum unfolding. Neutron cross section library was complied by the program CSTAPE which is a subprogram of the SAND II package. The 620 groups energy structure was applied in the calculations. The neutron cross sections for the library are given in **Table 2.3**. The guess spectrum[31] for neutron spectrum unfolding was one which was calculated with a one dimensional transport code ANISN[32]. The uncertainty of the guess spectrum was about ±30% from 0.3 to 3 MeV and about ±50% outside this range[31].

The unfolded neutron spectrum is shown in **Fig. 2.5**. The ratios of the measured reaction

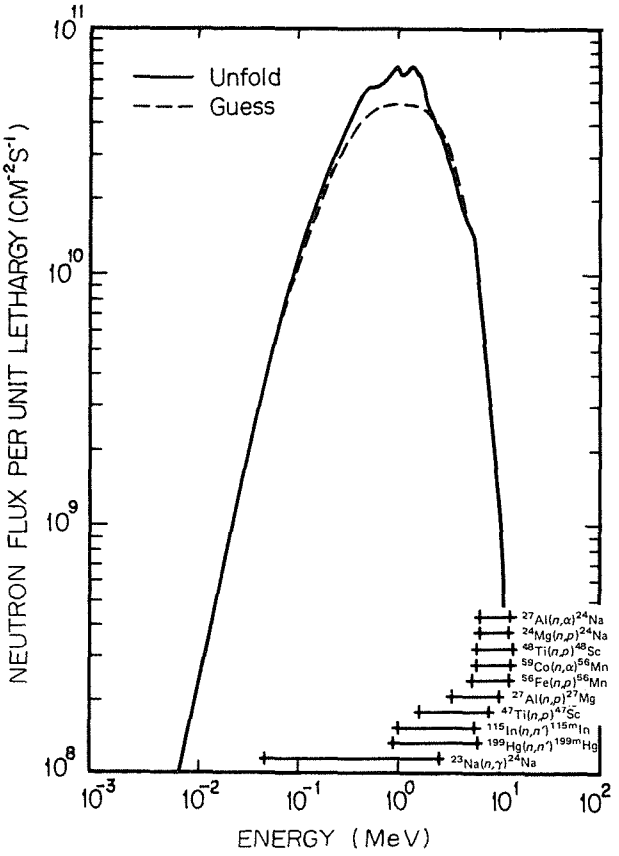

Fig. 2.5 Unfolded neutron spectrum of YAYOI glory-hole. (reactor power 500 W)

Table 2.4 Ratios of measured reaction rates to calculated ones after the zeroth and the final iterations in SAND II analysis

Reaction	Ratios of measured reaction rates to calculated ones	
	Guess spectrum	10 iteration spectrum
$^{59}Co(n,\alpha)^{56}Mn$	0.9582	1.0264
$^{56}Fe(n,p)^{56}Mn$	1.0144	1.0498
$^{27}Al(n,p)^{27}Mg$	1.0497	1.0750
$^{27}Al(n,\alpha)^{24}Na$	0.8895	0.9690
$^{24}Mg(n,p)^{24}Na$	0.9139	0.9850
$^{47}Ti(n,p)^{47}Sc$	0.8491	0.8721
$^{48}Ti(n,p)^{48}Sc$	0.8819	0.9463
$^{115}In(n,n')^{115m}In$	1.2210	1.1380
$^{23}Na(n,\gamma)^{24}Na$	1.2070	0.9941
$^{199}Hg(n,n')^{199m}Hg$	1.0164	0.9466

rates (M) to the calculated ones (C) are given in **Table 2.4**. The ratio in the zeroth and in the final iterations is given in the same table.

2.2.3 Results

More quantitative analysis will give information concerning the usefulness of the neutron dosimeter $^{199}Hg(n,n')^{199m}Hg$. Therefore, total neutron flux was calculated from the guess spectrum and from the unfolded spectrum. The values are 1.614×10^{11}, 1.826×10^{11} and 1.875×10^{11} n/cm^2·sec for the guess spectrum, the unfolded spectrum and the evaluated spectrum[28], respectively. The total neutron flux calculated from the unfolded spectrum with $^{199}Hg(n,n')^{199m}Hg$ reaction rate was 1% smaller than that without the reaction rate.

2.2.4 Discussion

The author has used natural mercury sample. Therefore, the activity of the ^{199m}Hg is produced by the $^{198}Hg(n,\gamma)^{199m}Hg$ and the $^{200}Hg(n,2n)^{199m}Hg$ reactions. As the neutron spectrum of the YAYOI glory-hole is very hard, the influence of the $^{198}Hg(n,\gamma)^{199m}Hg$ reaction is negligibly small. The fission spectrum averaged cross section of the $^{200}Hg(n,2n)^{199m}Hg$ reaction is 5.5 mb[33]. Therefore, the influence of the $^{200}Hg(n,2n)^{199m}Hg$ reaction is about 2%. The fission spectrum averaged cross section of the $^{199}Hg(n,p)^{199}Au$ reaction is 0.009 mb[33]. The influence of beta decay of the ^{199}Au is negligibly small.

The author had complied the neutron cross sections for the $^{199}Hg(n,n')^{199m}Hg$ reaction. One was complied by using the cross section data that were measured by Swann and Metzger[8], Bornemisza et al.[9] and Hankla et al.[11], another was complied by using the cross section data that were measured by Sakurai et al. (**2.1**) and Hankla et al.[11]. When the former cross sections are used for neutron spectrum unfolding, the ratio of measured reaction rate to calculated one for the zeroth iteration is about 3. The value is about $1 \sim 1.1$ when the latter cross sections are used for the unfolding.

The calculated fission spectrum averaged cross section is 238.3 mb. The half-life of the isomer is 42.6 minutes[7]. It means that the activity is easily produced by the irradiation with low level fast neutron flux. The author has used the reaction in the experiment at the critical assembly of the Japan Materials Testing Reactor. The threshold energy of the reaction is as low as that of the $^{115}In(n,n')^{115m}In$ reaction. Therefore, the $^{199}Hg(n,n')^{199m}Hg$, $^{115}In(n,n')^{115m}In$, $^{103}Rh(n,n')^{103m}Rh$ reactions should be useful neutron dosimeters for the neutron dosimetry with low level fast neutron flux.

3. Measurement of Neutron Fluence above 0.1 MeV with the Dosimeter $^{93}Nb(n,n')^{93m}Nb$

3.1 Impurities in the Niobium Wire

The niobium dosimeters used were wires 0.020 inches in diameter, 99.833% in purity, supplied by Reactor Experiments Inc. The impurities in the niobium wire are given in **Table 3.1** (Ref. 34). The abundance of ^{93}Nb is 100%. It is difficult to remove tantalum completely in the niobium wire. When the niobium wire is irradiated in a thermal neutron reactor such as the JMTR, ^{182}Ta with a half-life of 115 days[7] is produced by thermal neutron capture. The thermal neutron capture cross section is 21 barns[7]. Therefore, the activity of ^{182}Ta is larger than that of ^{93m}Nb produced by the $^{93}Nb(n,n')$ reaction. As a result, the measurement of KX-rays emitted from ^{93m}Nb is interfered with by KX-rays and gamma-rays from ^{182}Ta. When the niobium wire is covered by cadmium, the thermal neutron flux to the niobium wire is decreased. But the cadmium could not be used for the general irradiation experiment because the melting point of the cadmium is as low as 320.9°C.

Table 3.1 Impurities in Niobium Wire[34]

Impurity	Weight Percent	Impurity	Weight Percent
Carbon	0.001	Manganese	0.005
Oxygen	0.003	Calcium	0.001
Nitrogen	0.006	Aluminum	0.001
Hydrogen	0.0005	Copper	0.001
Tantalum	0.045	Tin	0.001
Tungsten	0.010	Chromium	0.005
Zirconium	0.020	Vanadium	0.010
Molybdenum	0.010	Cobalt	0.002
Titanium	0.010	Hafnium	0.010
Iron	0.005	Cadmium	0.005
Nickel	0.005	Lead	0.005
Silicon	0.005		

3.2 Irradiation of Niobium Wire in JMTR

The JMTR is a high-flux reactor with a thermal power of 50 MW. About 60 fuel and material capsules have been irradiated in the core for each cycle. The core of JMTR is shown in **Fig. 3.1**. The maximum thermal neutron flux is 4×10^{14} n/cm^2·sec at the first beryllium reflector region. The maximum fast neutron flux above 1 MeV is 4×10^{14} n/cm^2·sec at the fuel region.

Niobium wires were irradiated at the irradiation hole J-12 of the second beryllium reflector region as shown in **Fig. 3.1**. The niobium wires of ~1.6 mg were set in the material capsule, which was scheduled to be irradiated at the irradiation hole J-12. The iron wires of ~1 mg were also set at the same position as niobium wires in the capsule.

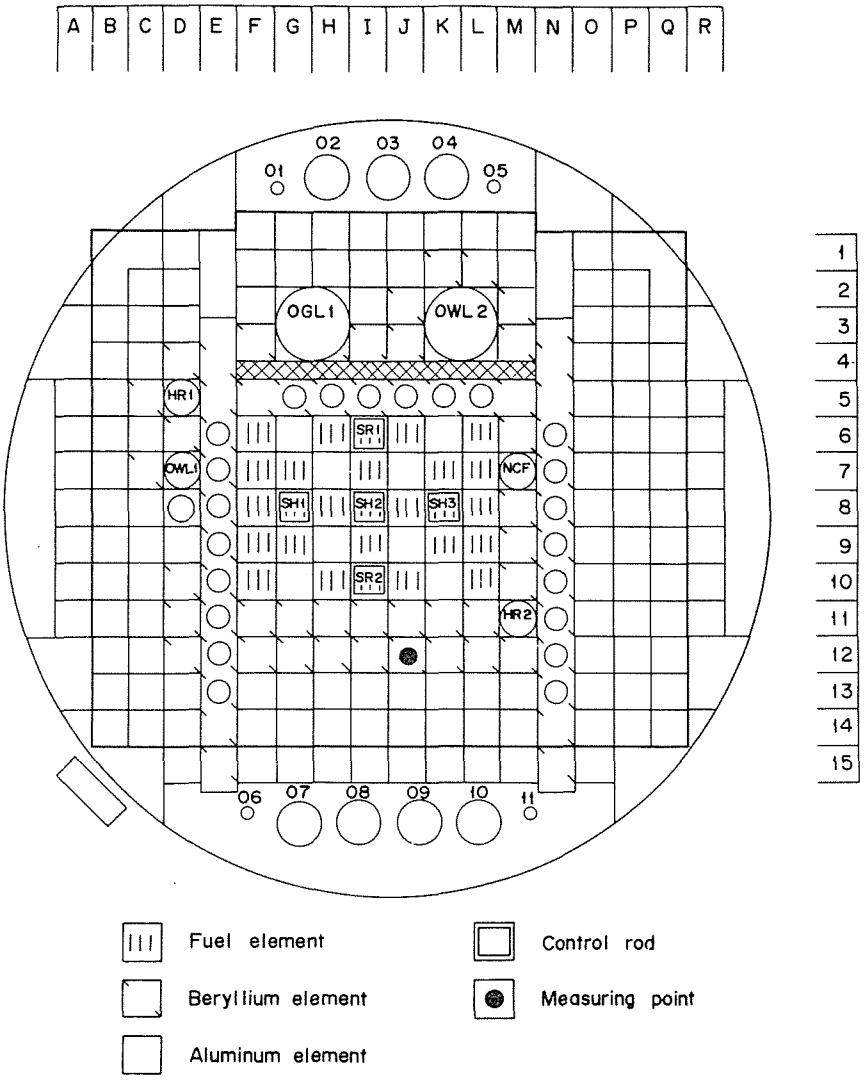

Fig. 3.1 The JMTR core.

The reason the irradiation hole J-12 was selected is that the ratio of thermal neutron flux to fast neutron flux is largest in the second beryllium reflector region. The ratios are ~2.2, 5.4, and 3.8 for the first and second beryllium reflector regions and the first aluminum reflector region, respectively. When the niobium wire is irradiated in the neutron field with high thermal neutron flux, ^{182}Ta is produced by the thermal neutron capture, and the measurement of KX-rays emitted from ^{93m}Nb is interfered with by KX-rays and gamma-rays from ^{182}Ta. If the niobium wire is irradiated in the neutron field with the highest ratio of thermal neutron flux to fast neutron flux, the result is applied to other irradiation holes in the JMTR core and other reactor. When the activity of ^{93m}Nb was measured without chemical separation after one year cooling period, it was an important point to know whether the measurement of ^{93m}Nb is accurate enough or not.

The niobium dosimeters were irradiated during the 45th cycle (January 13 to February 16, 1979), the 46th cycle (March 29 to April 24, 1979), and the 47th cycle (June 17 to July 13, 1979).

3.3 Measurement of KX-rays emitted from ^{93m}Nb with High Purity Germanium detector

The transition from ^{93m}Nb is classified to M4, which means ~100% internal conversion. Gamma-rays emitted from ^{182}Ta in the niobium dosimeter were measured with a 110 cm^3 Ge(Li) detector after 412 days of cooling time. The gamma-ray spectrum is shown in **Fig. 3.2**. The 1.614 mg niobium wire on the Mylar film was dissolved by slowly adding a few drops of HNO_3 and HF mixture. The X-ray self-absorption is negligibly small for the X-ray source. The KX-rays emitted from ^{93m}Nb after 415 days of cooling time were measured with a high-

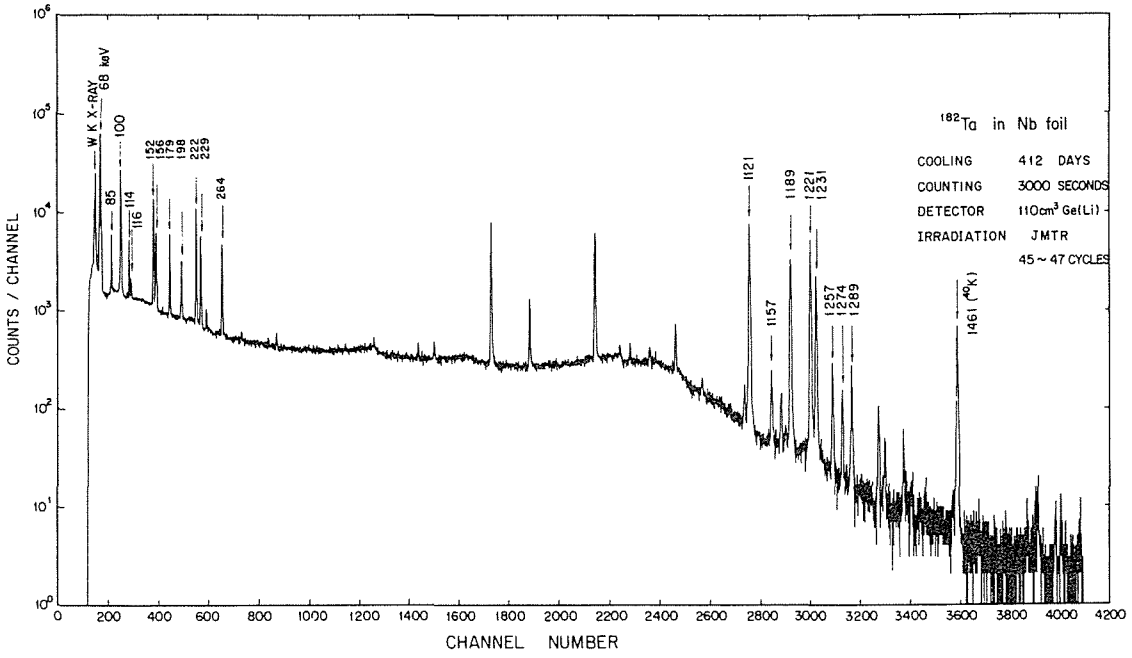

Fig. 3.2 Gamma-ray spectrum of ^{182}Ta in the niobium dosimeter after 412 days of cooling time.

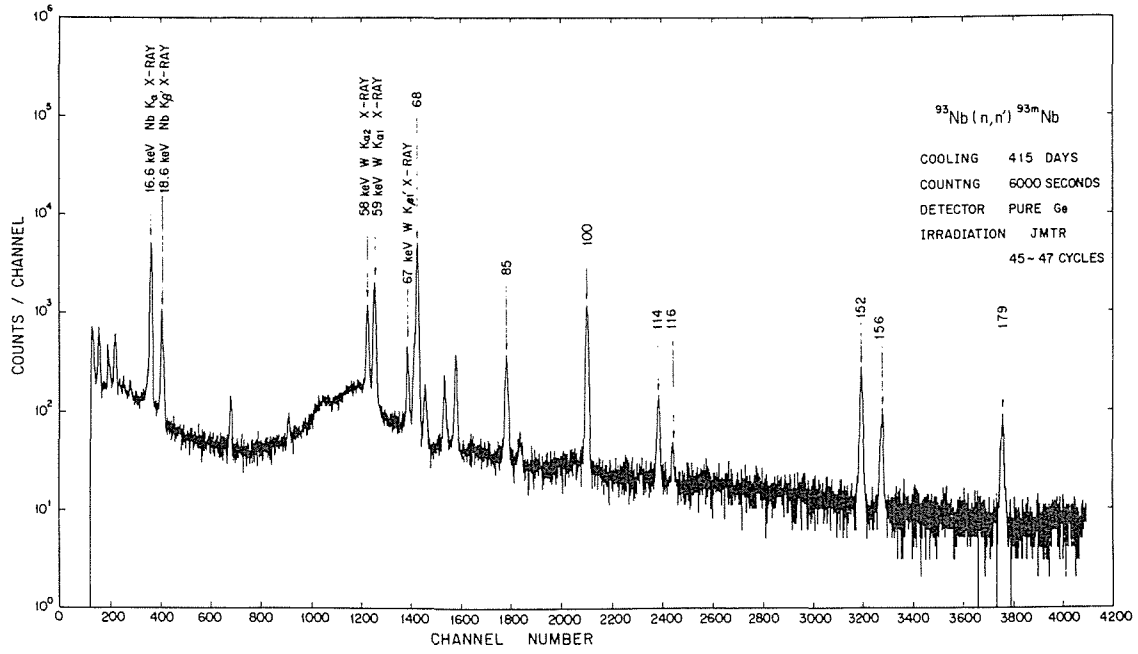

Fig. 3.3 KX-ray spectrum of ^{93m}Nb after 415 days cooling time.

purity 200 mm^2 X 7 mm germanium detector. The KX-ray spectrum is shown in **Fig. 3.3**. The low energy region of ^{182}Ta is also shown. The KX-ray spectrum of ^{93m}Nb is slightly interfered with by KX-rays and gamma-rays from ^{182}Ta. It is possible to determine the peak area with high accuracy when the explicit KX-ray peak as shown in **Fig. 3.3** is obtained. KX-rays of ~50000 counts were detected at a distance of 10 cm between the detector and the source for the counting time of 6000 seconds. The detection efficiency of the high-purity germanium detector was determined by using a ^{241}Am standard source. The data of the half-life and the branching ratio in Ref. 7 were used.

3.4 Evaluation of Neutron Fluence above 0.1 MeV

The neutron fluence above 0.1 MeV is strictly calculated from the data of the absolute activity determined by KX-ray measurement, the neutron spectrum, the $^{93}Nb(n,n')^{93m}Nb$ cross section, the irradiation time, the cooling time, the half-life, and the branching ratio of ^{93m}Nb. The neutron fluence is expressed in the following equation:

$$\Phi = A \frac{M}{N_o m a} \frac{1}{\sigma_{0.1}} \frac{\sum_{j=1}^{n} t_{ij}}{\sum_{j=1}^{n} (1-e^{-\lambda t_{ij}}) e^{-\lambda t_{wj}}} \tag{3.1}$$

where Φ : neutron fluence above 0.1 MeV (n/cm^2)
A : activity (dps)
M : atomic weight for dosimeter (amu)
N_o : Avogadro number (6.022×10^{23} $mole^{-1}$)
m : dosimeter weight (g)
a : abundance
$\sigma_{0.1}$: effective cross section above 0.1 MeV (cm^2)
t_i : irradiation time (sec)
λ : decay constant (sec^{-1})
t_w : cooling time (sec)
n : irradiation cycle

The effective cross section above 0.1 MeV of the $^{93}Nb(n,n')^{93m}Nb$ reaction is defined by the following equation:

$$\sigma_{0.1} \equiv \frac{\int_0^\infty \phi(E)\sigma(E)dE}{\int_{0.1}^\infty \phi(E)dE} \tag{3.2}$$

where $\phi(E)$ is the neutron spectrum and $\sigma(E)$ is the $^{93}Nb(n,n')^{93}Nb$ cross section.

The data used are the half-life of 13.6 ± 0.3 years[7] and branching ratio of 0.116 ± 0.0035[35]. The neutron spectra were calculated by using the ANISN code with the slab model for the JMTR core[36]. The $^{93}Nb(n,n')^{93m}Nb$ cross section determined by Hegedüs[37] was used to calculate the effective cross section above 0.1 MeV. The $^{93}Nb(n,n')^{93m}Nb$ cross section curve is shown in **Fig. 3.4**. Hegedüs used the half-life of 11.4 years and the branching ratio of 0.122[37]. The relation of the present nuclear data [the cross section $\sigma(E)$, the half-life $T_{1/2}$, and the branching ratio I_{KX}] and the nuclear data used by Hegedüs [the cross section $\sigma'(E)$, the half-life $T'_{1/2}$, and the branching ratio I'_{KX}] is expressed by the following equation[38]:

$$\sigma(E) = \frac{T_{1/2}}{I_{KX}} \frac{I'_{KY}}{T'_{1/2}} \sigma'(E) = \frac{13.6}{0.116} \frac{0.122}{11.4} \sigma'(E) = 1.25\sigma'(E) \tag{3.3}$$

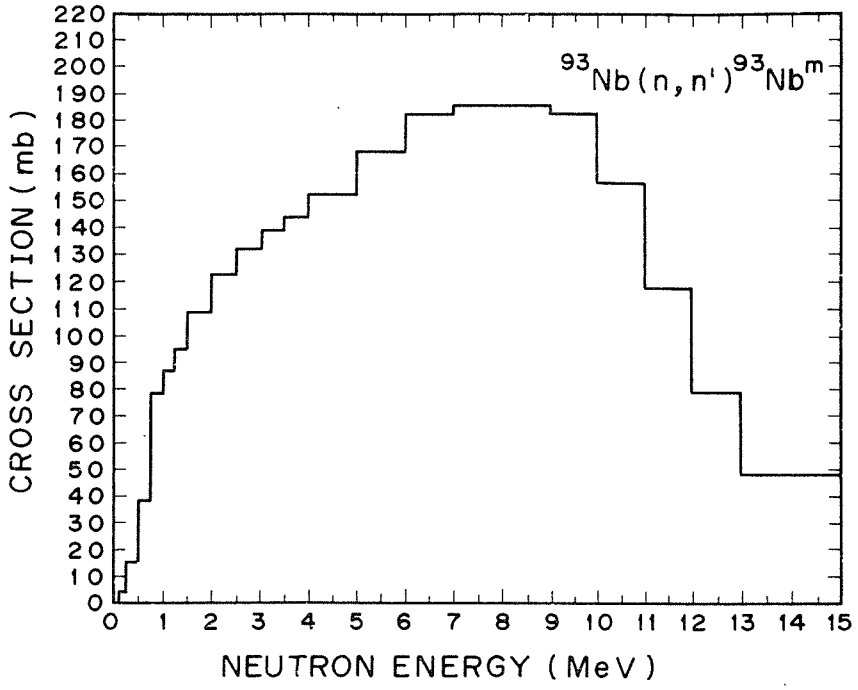

Fig. 3.4 $^{93}Nb(n,n')^{93m}Nb$ cross section curve determined by Hegedüs[37].

The $\sigma_{0.1}$ for the $^{93}Nb(n,n')^{93m}Nb$ reaction is 75.2 mb. The $\sigma_{0.183}$ was also calculated in order to compare with the neutron fluence above 0.183 MeV calculated for the JMTR core[36], and the value is 84.7 mb.

The accuracy of the neutron fluence above 0.183 MeV can be evaluated by comparison with the neutron fluence above 0.183 MeV monitored with the dosimeters and that calculated for the JMTR core. The effective cross section of the $^{54}Fe(n,p)^{54}Mn$ reaction was calculated by using the ANISN spectrum and the $^{54}Fe(n,p)^{54}Mn$ cross section in ENDF/B-IV. The values are 25.8 and 29.9 mb for above 0.1 and 0.183 MeV, respectively.

3.5 Results

The neutron fluence above 0.1 and 0.183 MeV monitored with dosimeters and the neutron fluence above 0.183 MeV calculated for the JMTR core are given in **Table 3.2**. The neutron fluence above 0.183 MeV monitored with the niobium dosimeter is 23% larger than that monitored with the iron dosimeter and that calculated for the JMTR core. The neutron fluence above 0.1 MeV measured with the niobium dosimeter is also 23% larger than that monitored with the iron dosimeter. The uncertainty of the neutron spectrum is experimentally

Table 3.2 Neutron fluence above 0.1 and 0.183 MeV monitored with the dosimeters $^{93}Nb(n,n')^{93m}Nb$ and $^{54}Fe(n,p)^{54}Mn$, and neutron fluence above 0.183 MeV calculated for JMTR core

Method	>0.183 MeV (n/cm^2)	>0.1 MeV (n/cm^2)
JMTR calculation	2.21×10^{20}	
$^{54}Fe(n,p)^{54}Mn$	2.12×10^{20}	2.46×10^{20}
$^{93}Nb(n,n')^{93m}Nb$	2.61×10^{20}	3.03×10^{20}

evaluated at ±20% for energy from 0.1 to 10 MeV[39]. The uncertainty of the neutron fluence above 0.1 MeV measured with the dosimeter $^{93}Nb(n,n')^{93m}Nb$ is smaller than ±30% including the uncertainties of the half-life, the branching ratio, the $^{93}Nb(n,n')^{93m}Nb$ cross section and the ANISN spectrum. The burnup of ^{93}Nb and ^{93m}Nb is negligibly small in this irradiation.

3.6 Discussion

The uncertainties are ~2, 3, 10 and 20% for the half-life, the branching ratio, the activity measurement, and the effective cross section above 0.1 MeV for the $^{93}Nb(n,n')^{93m}Nb$ reaction, respectively. The uncertainty of the neutron fluence above 0.183 MeV with the niobium dosimeter indicates a disagreement with the iron dosimeter and the nuclear calculation[36].

The cadmium thermal neutron filter could not be used because of the low melting point, but one can use CdO up to 900°C, which is routinely used in Westinghouse pressurized water reactors. However, the ideal filter to reduce ^{181}Ta activation is a 0.5 mm thick CdO and a 0.15 mm thick tantalum metal. The tantalum absorbs the 4.3 eV neutrons, reducing to practically zero the resonance activation in tantalum.

The quality of the niobium wire, which contains 450 ppm tantalum, is very bad. Currently available on the market is: 250 ppm for metals and 80 ppm for Nb_2O_5 powder, but for a higher price one can buy 5 ppm quality metal too.

The fluorescence effect of ^{182}Ta in the niobium depends on the sample thickness and the $^{182}Ta/^{93m}Nb$ activity ratio. In this study, ~30% of the niobium KX-rays was due to the fluorescence of the ^{182}Ta gamma-rays in the niobium K-shell. This correction was applied to the activity determination of the ^{93m}Nb.

The neutron fluence above 0.1 MeV with the niobium dosimeter was measured and the following problems were explicated:

1) The measurement of KX-rays emitted from ^{93m}Nb is possible without the chemical separation of ^{182}Ta activity and ^{93m}Nb activity.
2) The niobium wire, ~1.6 mg, is dissolved by slowly adding a few drops of HNO_3 and HF mixture, and the preparation of the KX-ray source with small self-absorption is possible.
3) The uncertainty of the neutron fluence above 0.1 MeV measured with the dosimeter $^{93}Nb(n,n')^{93m}Nb$ is smaller than 30%, including the uncertainties of the half-life, the branching ratio, the $^{93}Nb(n,n')^{93m}Nb$ cross section, and the neutron spectrum.

4. Use of New Dosimeter $^{107}Ag(n,n')^{107m}Ag$ for Neutron Spectrum Unfolding

4.1 Method of Study

Natural silver is made up of 51.83% ^{107}Ag and 48.17% ^{109}Ag, which produce their respective isomers through (n,n') reaction. Generally speaking, the cross section of an (n,n') reaction for isomer generation is constituted of a number of inelastic scattering cross sections each corresponding to its own excitation energy. And in the present case, no published data are available on the individual cross sections for the $^{107}Ag(n,n')^{107m}Ag$ and $^{109}Ag(n,n')^{109m}Ag$ reactions. The inelastic scattering cross sections for ^{107}Ag and ^{109}Ag, on the other hand, are found in ENDF/B-IV, each representing itself for every excitation energy (−Q value), as given by Baht & Prince[40]. Beyond the absolute Q value, these cross sections are treated as continuum. The contribution of this continuum region to isomer production is unknown for ^{107}Ag and ^{109}Ag. The author has derived the cross section of the $^{107}Ag(n,n')^{107m}Ag$ reaction by compilation from the ENDF/B-IV and the "Table of Isotopes"[7].

The decay scheme of ^{107}Ag from its excitation levels[7] is presented in **Fig. 4.1**, while **Fig. 4.2** shows the excitation cross section curves, together with the complied isomer production cross section curve in dashed line. In ENDF/B-IV, the excitation levels of ^{107}Ag above 0.9497 MeV are classed in the continuum region, which leaves some ambiguity concerning the contribution of these levels to the production of ^{107m}Ag. In order to eliminate this ambiguity through experimental evaluation, a 99.0% ^{107}Ag enriched Ag-foil was irradiated, in company with several reference foils, in the glory-hole of YAYOI, which served as the standard neutron field[28], the neutron spectrum through this glory-hole having been the subject of thorough survey[28], with the result shown in **Fig. 4.3**[28].

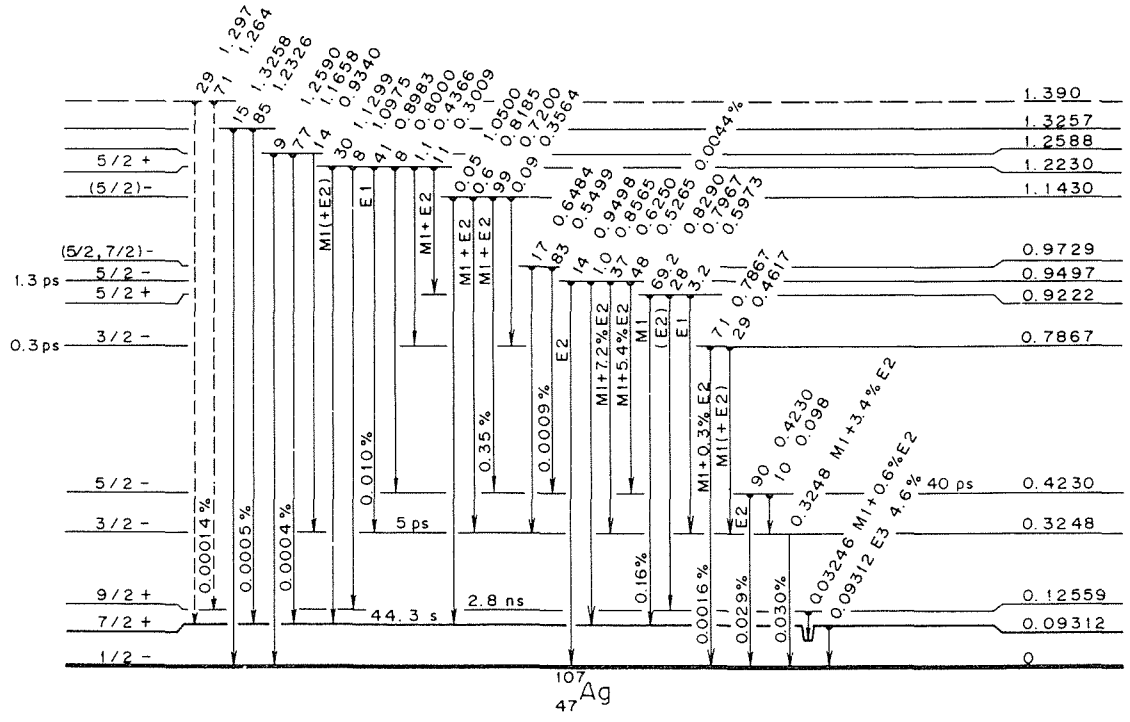

Fig. 4.1 Excited State of ^{107}Ag[7].

The validity of the derived $^{107}Ag(n,n')^{107m}Ag$ reaction cross section was examined in terms of: (1) whether the compiled cross section could reliably serve for reference in isomer production, and (2) whether the process envisaged for monitoring isomer production would be appropriate, including the techniques for activity measurement (KX-ray counting, evaluation of isotope data et.). To determine these points, the following procedure was adopted: (1) irradiation of ^{107}Ag-foil in company with several reference foils in the core-center of YAYOI, (2) unfolding with the spectrum in **Fig. 4.3** as the guess spectrum, (3) comparison of

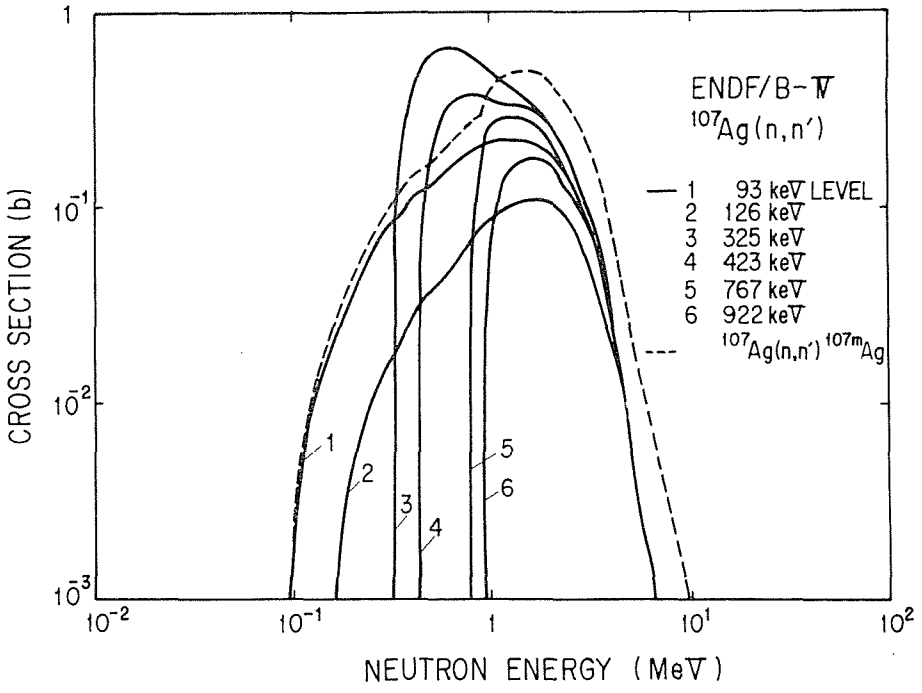

Fig. 4.2 Inelastic scattering cross sections of $^{107}Ag(n,n')$ reaction and isomer production cross section.

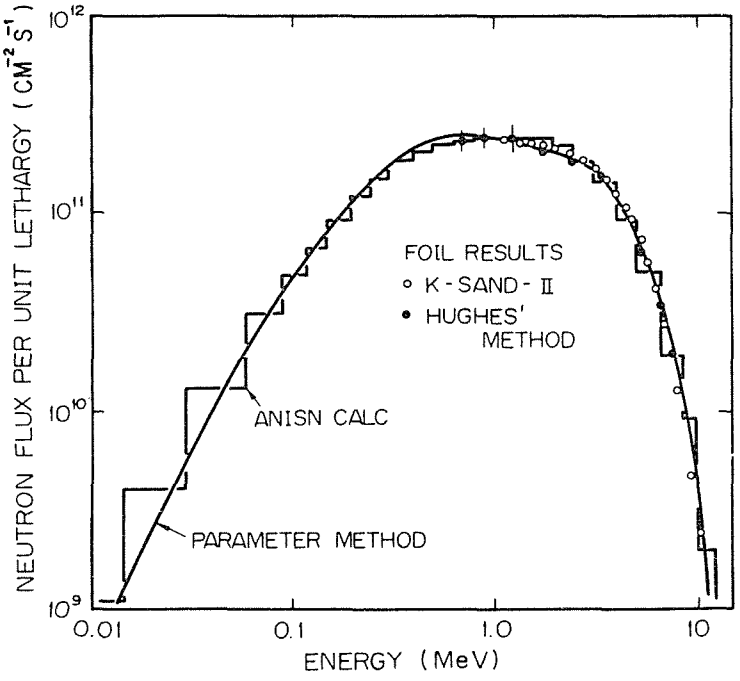

Fig. 4.3 Neutron spectrum at core-center of YAYOI[28] (Reactor power 2 kW).

the unfolded spectrum with the initial spectrum to examine whether the influence of ^{107}Ag-foil on the spectrum exceeds experimental error and that previously included in the initial spectrum.

4.2 Foil Irradiation in YAYOI

The neutron spectrum measurements in the core-center of YAYOI adopted as standard neutron field were performed using the nuclear reactions ^{197}Au$(n,\gamma)^{198}$Au, ^{55}Nn$(n,\gamma)^{56}$Mn, ^{103}Rh$(n,n')^{103m}$Rh, ^{56}Fe$(n,p)^{56}$Mn, ^{48}Ti$(n,p)^{48}$Sc, ^{27}Al$(n,\alpha)^{24}$Na, ^{24}Mg$(n,p)^{24}$Na and ^{107}Ag(n,n') ^{107m}Ag. Except for the ^{107}Ag-foil, all the neutron dosimeter foils were irradiated for 30 minutes at 500 W. The ^{107}Ag-foil was irradiated three times at 3, 30 and 100 W, each for 10 minutes.

In the YAYOI core-center, the foil was suspended with string from the top of the vertical hole (glory-hole) which penetrates the core-center. Correct positioning of the foil in core-center was verified by observing the reactivity changes accompanying small changes in foil position at low reactor power; the string was then marked where it passed the top of the glory-hole, as reference indication for purposes of reproducibility between different runs. A weight was attached to the lower end of the string, at a length of 10 cm from the foil so as not to disturb the neutron field under measurement.

4.3 Measurement of Induced Activity

The induced activity of the irradiated foils was measured with a 110 cm^3 Ge(Li) detector or else with a high-purity germanium detector, depending on whether gamma- or KX-ray was to be counted. The activity of isomers such as ^{103m}Rh and ^{107m}Ag was measured by X-ray counting with the high-purity germanium detector. In both cases, the K_α and K_β' X-ray peaks were used for determining the activity. Silver presents X-ray energies of K_α 22 keV and K_β' 25 keV, which both require the foil to be thin enough to be free from self-absorption effect. This was realized by letting the foil take the form of silver nitrate coating on a polyethylene film support, which reduced the self-absorption below 1%. The ^{107}Ag$(n,n')^{107m}$Ag reaction rate was determined by KX-ray and 93 keV gamma-ray counting with the high-purity germa-

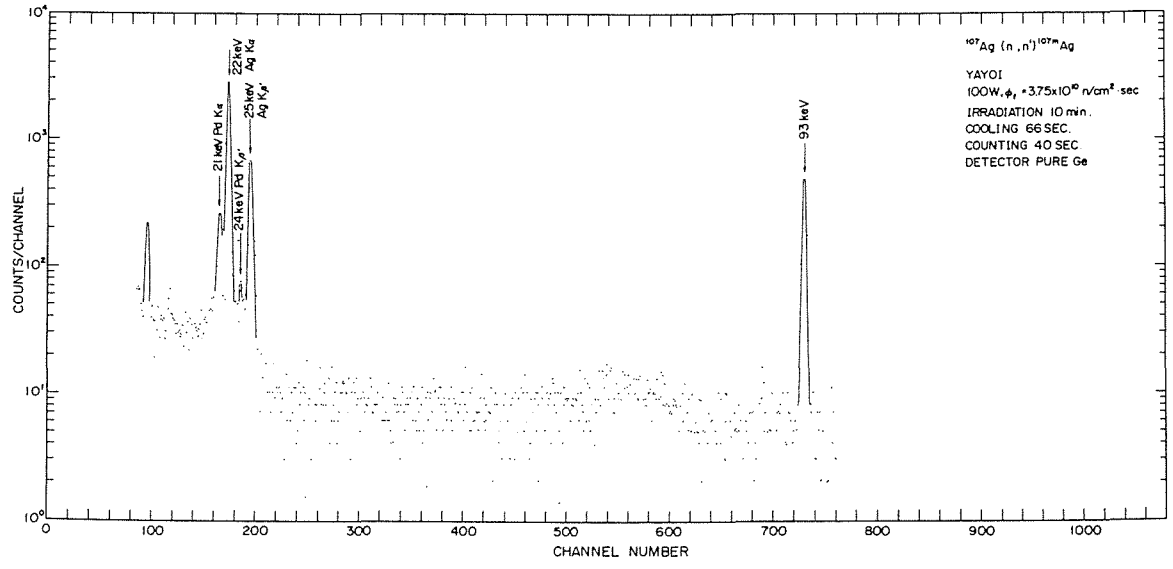

Fig. 4.4 X- and gamma-ray spectra from ^{107}Ag.

nium detector.

A 1 μCi ^{241}Am standard source was made to serve for the energy and efficiency calibrations. For counting the 93 keV gamma-ray from ^{107m}Ag, the absolute efficiency curve was determined by reference to the 60 keV gamma-ray of ^{241}Am, the 122 keV gamma-ray of ^{57}Co, and 66, 97, 121 and 136 keV gamma-rays of ^{75}Se. The decay data were referred to Ref. 7.

Figure 4.4 represents the spectra of the X- and gamma-rays from the ^{107}Ag-foil that was irradiated for 10 minutes at 100 W. The foil was there after cooled down for 66 seconds, and counted for 40 seconds. **Figure 4.5** represents only the X-ray spectrum from ^{107m}Ag.

4.4 Results

The reaction rates obtained from the foil activity measurements are presented in **Table 4.1**. These results were compared with those of other foil irradiations performed in the same YAYOI core-center by three other groups – from the Nuclear Engineering Research Laboratory of the University of Tokyo, the Kyoto University Reactor Research Institute, and the Power Reactor and Nuclear Fuel Development Corp.[29]. The comparison revealed discrepancies that did not exceed ±2~3% in respect of the individual reaction rate of all foils except Ti.

The foil activity comparison between Ag and the references was made using the YAYOI glory-hole, whose neutron spectrum had been accurately evaluated by repeated measurements and by calculation[28]. The activation cross sections of the reference foils were taken from

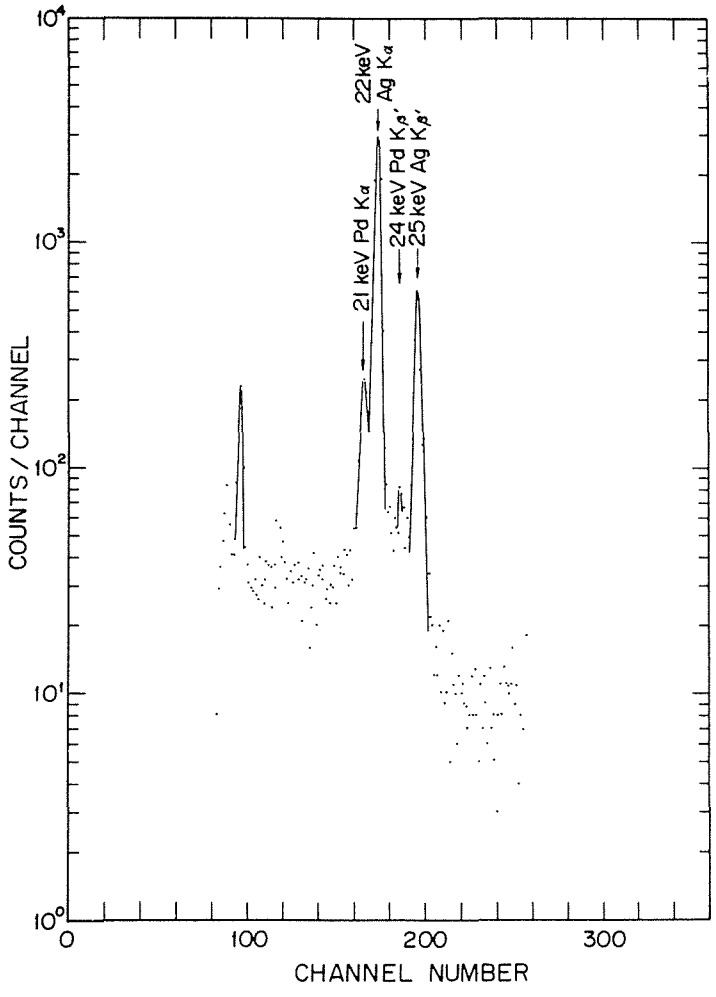

Fig. 4.5 X-ray spectrum for ^{107m}Ag (after 67 sec cooling, 40 sec counting).

Table 4.1 Reaction rates of foils irradiated in TAYOI glory-hole at 500 W power

Foil	Reaction	Abundance(a)	$T_{1/2}$(b)	Eγ(keV)(b)	Branching (%)(b)	Reaction rate (dps/atom)
Mg	$^{24}Mg(n,p)^{24}Na$	78.99	15.030 h	1,368	100	1.40−16+
Al	$^{27}Al(n,\alpha)^{24}Na$	100	"	"	"	6.91−17
Ti	$^{48}Ti(n,p)^{48}Sc$	73.7	43.67 h	983	"	3.08−17
Mn	$^{55}Mn(n,\gamma)^{56}Mn$	100	2.579 h	846	98.8	8.23−16
Fe	$^{56}Fe(n,p)^{56}Mn$	91.7	"	"	"	1.04−16
Rh	$^{103}Rh(n,n')^{103m}Rh$	100	56.116 min	KX-ray 20,23	7.0	6.06−14
Ag (enriched)	$^{107}Ag(n,n')^{107m}Ag$	"	44.3 s	KX-ray 22,25	35.5	3.56−14
Au	$^{197}Au(n,\gamma)^{198}Au$	"	2.697 d	412	95.5	3.14−14

(a) "Nuklidkarte", (1974), (b) "Table of Isotopes", (1978).
\+ 1.40−16 means 1.40×10^{-16}.

ENDF/B-IV. The data comparison was performed by means of the unfolding code SAND II[30], with the measured foil activity values as input, the known glory-hole neutron spectrum as guess spectrum.

The interim result after zeroth iteration of the unfolding process is given in **Table 4.2**. This table represents the deviations of the individual foil activities from what should have been if the corresponding initial spectra were true. It is seen from this table that the smallest deviation is the 4.24% shown by Ag, which appears to be a reasonable value in comparison with the corresponding deviations of the other seven reference foils. The neutron spectrum unfolded with DAND II is shown in **Fig. 4.6**. Exclusion of Mn and Au from the reference foils – on account of the uncertainty of their spectra in the lower extremity of the energy range – results in some increase of deviation of the Ag-foil. This deviation was examined by scrutinizing the activity of the Rh-foil, which has its sensitive range closest to that of Ag (see **Table 4.2**). Also, the cross section of Fe was recomplied from ENDF/B-V to remedy the deviation which was much larger than seen for the other four reference foil activities. These corrective measures brought the deviation of the Ag-foil activity from those of the other five references down to 12.8%. The corresponding deviations of the other references were −3.4 for the Mg, −8.9 for the Ti, −5.2 for the Al, −5.3 for the Rh and 9.9% for the Fe-foil activities.

Table 4.2 Interim results obtained at zeroth iteration of unfolding analysis

Foil reaction	Nominal 5% activity limites (MeV)		Ratio measured to calculated activities	Deviation of measured from calculated activity (%)
	Lower	Upper		
$^{197}Au(n,\gamma)^{198}Au$	4.50−2+	1.90	1.1091	10.91
$^{24}Mg(n,p)^{24}Na$	6.80	1.37+1	0.8926	−10.74
$^{48}Ti(n,p)^{48}Sc$	7.30	1.51+1	0.8423	−15.77
$^{56}Fe(n,p)^{56}Mn$	5.70	1.36+1	1.1133	11.33
$^{27}Al(n,\alpha)^{24}Na$	6.90	1.39+1	0.8762	−12.38
$^{103}Rh(n,n')^{103m}Rh$	5.00−1	5.10	0.8757	−12.43
$^{107}Ag(n,n')^{107m}Ag$	4.00−1	2.60	1.0424	4.24
$^{55}Mn(n,\gamma)^{56}Mn$	3.00−2	2.20	1.2484	24.84

Standatd deviation of activities: 14.90%
\+ 4.50−2 means 4.50×10^{-2}.

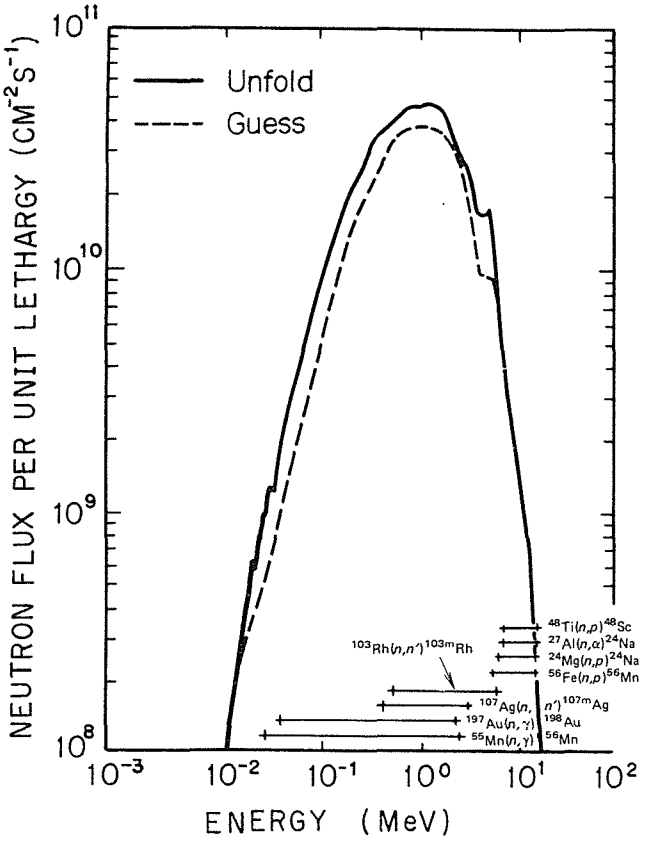

Fig. 4.6 Neutron spectrum unfolded by means of SAND II. (YAYOI glory-hole, reactor power 500 W)

4.5 Discussion

Uncertainty in the calculation of activity caused by the precision of the cross section for $^{107}Ag(n,n')^{107m}Ag$ reaction was estimated to be 12.8% from the following treatment.

The foil irradiation flux level that is determined by the five references is, in principle, represented by

$$X = \mu + \sigma_X$$

where μ denotes the most probable value of the flux level, and σ_X the standard deviation obtained by the equation

$$\sigma_x = \sqrt{\sum_{i=1}^{N} \sigma_{xi}^2 \Big/ (N-1)}$$

where again σ_{xi} represents the deviation of the i-th reference activity from the expected value calculated using the most probable level of flux with the given spectrum. The five selected reference activities give 2.12% for σ_x. And μ itself carries a certain ambiguity resulting from the uncertainties contained in the activities of the five foils:

$$\mu = \mu_0 + \sigma_\mu$$

where the uncertainty σ_μ is represented by

$$\sigma_\mu = \sqrt{1 \Big/ \sum_i \frac{1}{\sigma_i^2}}$$

where again σ_i denotes the uncertainty of the i-th reference activity due to its uncertainties

such as deriving from decay data, activity counting efficiency and counting error. For all five references, σ_i is estimated to be 5%, which yields 2.50% for σ_μ. Based on these values of uncertainty, that of the flux level at which the Ag-foil has been irradiated is estimated to be $\sigma_x + \sigma_\mu = 4.62\%$.

In the estimation of Ag-foil activity, uncertainties of various contributions were evaluated:

1) counting efficiency of the Ge detector = 3%,
2) decay data = 1%,
3) counting statistics = 1%,
4) correction of X-ray absorption = 1%.

The sum of these uncertainties are well within the uncertainty value 12.8% quated above.

Figure 4.7 represents the response functions $\sigma(E)\phi(E)$ ($\sigma(E)$: cross section, $\phi(E)$: neutron spectrum) of ^{107}Ag-foil derived from spectra obtained in the YAYOI glory-hole and in the first Be reflector of JMTRC[36]. Both curves indicate a foil response contribution of about 30% provided in the energy range of 0.1～1 MeV, where the integral neutron flux is more than twice that above 1 MeV.

The range of 0.1～1 MeV, on the other hand, is precisely the region where no neutron dosimeters have their peak sensitivity, so that spectrum measurements in this region must be considered to generate the bulk of the activity error: If a combination of foils is used such as to constitute too many neutron dosimeters sensitive in the higher energy range, this would tend to magnify this error. As a practical example, the influence imparted by the error of ^{107}Ag activity on the JMTRC spectrum was studied in reference to the reactions ^{103}Rh$(n,n')^{103m}$Rh, ^{238}U(n,f)FP, ^{115}In$(n,n')^{115m}$In, ^{55}Mn$(n,\gamma)^{56}$Mn and ^{63}Cu$(n,\gamma)^{64}$Cu, which gave the results tabulated below.

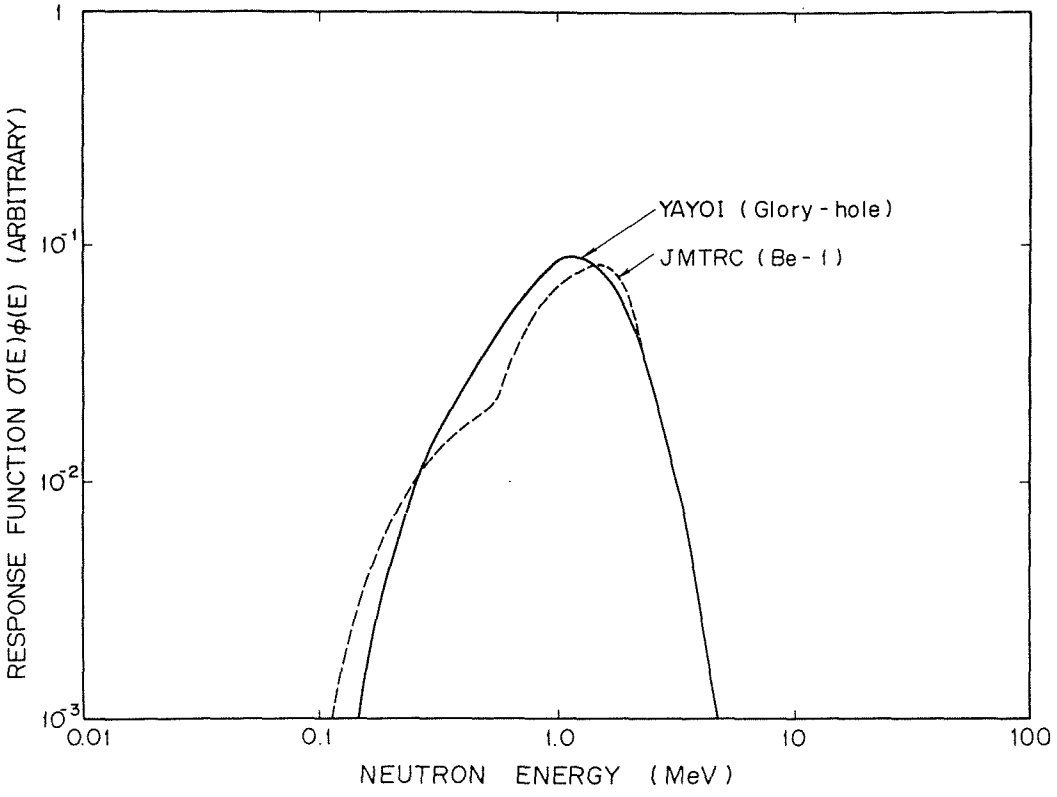

Fig. 4.7 Response functions of ^{107}Ag foil obtained with YAYOI glory-hole spectrum and spectrum at JMTRC first beryllium reflector.

Ag activity change (%)	Flux level change (%)
	(Normalized to flux > 1 MeV)
−10	−15.8 (at 0.38 MeV)
+10	5.7 (at 0.40 MeV)

The reason for difference seen in the extent of change brought in the flux level for an equal amount of Ag activity in opposite directions can be attributed to the difference of the spectrum adopted with 5% standard deviation as condition of convergence. Considering these changes brought on the spectrum to represent maximum values, it can be concluded that a change of 10% in Ag activity should bring about a change in flux level of roughly same amount.

5. Conclusion

An important point requiring consideration in studying radiation damage for reactor materials is neutron dosimetry with 0.1～1 MeV range. New dosimeters $^{199}Hg(n,n')^{199m}Hg$, $^{93}Nb(n,n')^{93m}Nb$ and $^{107}Ag(n,n')^{107m}Ag$ were studied to measure neutron with energy from 0.1 to 1 MeV. As a result, the following conclusion is obtained.

1) Neutron cross sections for the $^{199}Hg(n,n')^{199m}Hg$ reaction were measured at 10 energy points from 0.78 to 6.3 MeV by the activation method. The neutron flux was determined with a proton recoil telescope counter and indium foils. The experimental errors for the neutron cross sections are about 11～19% for the indium neutron flux monitoring and 5～8% for the proton recoil neutron flux monitoring. The neutron cross sections determined with two methods agree within the experimental error. It means that the neutron cross sections do not include the systematic error. For the use of the present data in the neutron dosimetry experiment, the present data and Hankla's data[11] were fitted with an empirical formula shown by Cross and Ing[24]. The fission spectrum averaged cross section for the Watt type spectrum is about 5% smaller than the measured one. It means that the accuracy of the neutron cross sections is enough for application in reactor neutron dosimetry.

2) The validity of the dosimeter $^{199}Hg(n,n')^{199m}Hg$ was examined through an irradiation experiment using the standard neutron field in the YAYOI. The neutron spectrum was unfolded with SAND II using 10 reaction rates including the dosimeter $^{199}Hg(n,n')^{199m}Hg$. The unfolded spectrum agrees with the evaluated spectrum[28]. The total neutron flux calculated from the unfolded spectrum with $^{199}Hg(n,n')^{199m}Hg$ reaction rate was 1% smaller than that without the reaction rate. New dosimeter $^{199}Hg(n,n')^{199m}Hg$ becomes a useful neutron dosimeter for neutron spectrum unfolding.

3) The neutron fluence above 0.1 MeV was measured with the dosimeter $^{93}Nb(n,n')^{93m}Nb$ at the irradiation hole J-12 of the second beryllium reflector region in the JMTR. The $^{93}Nb(n,n')^{93m}Nb$ cross section determined by Hegedüs[37] was used to calculate the effective cross section above 0.1 MeV. The uncertainty of the neutron fluence above 0.1 MeV is smaller than 30%, including the uncertainties of the nuclear data and the neutron spectrum.

4) The validity of the dosimeter $^{107}Ag(n,n')^{107m}Ag$ was examined through an irradiation experiment using the standard neutron field in the YAYOI, a fast neutron source reactor. The test foil used was 99.0% ^{107}Ag enriched silver, which was irradiated with 5 reference foils already well evaluated. The reaction rate of ^{107}Ag was determined by KX-ray counting with a high-purity germanium detector. The cross section for the $^{107}Ag(n,n')^{107m}Ag$ reaction was compiled from the excitation cross section data of ^{107}Ag published in ENDF/B-IV, in combination with the decay scheme of ^{107m}Ag listed in the "Table of Isotopes". Using the neutron spectrum which had previously been precisely measured, it was found that the calculated reaction rate of ^{107m}Ag was underestimated by 12.8 ± 5%. This error is attributed to significant underestimation involved in the cross section of the $^{107}Ag(n,n')^{107m}Ag$ reaction.

Acknowledgement

The author would like to express his grateful acknowledgement to Dr. I. Kondo at the Japan Atomic Energy Research Institute for his helpful discussion on reactor neutron dosimetry and neutron spectrum unfolding. Grateful appreciation is expressed to Prof. Dr. M. Nakazawa and Prof. Dr. A. Sekiguchi at the University of Tokyo for their discussion on reactor neutron dosimetry.

The author would like to express his grateful acknowledgement to Prof. Dr. H. Yamaguchi at Science University of Tokyo for advice on preparing this manuscript. Sincere thanks are also expressed to Prof. Dr. Y. Makita, Prof. Dr. T. Sekigawa and Prof. Dr. K. Yamamoto at Science University of Tokyo for their helpful support for this work.

References

1) Proc. 1st ASTM-EURATOM Symp. Reactor Dosimetry, EUR-5667 (1977).
2) Proc. 2nd ASTM-EURATOM Symp. Reactor Dosimetry, NUREG/CP-0004 (1979).
3) Proc. 3rd ASTM-EURATOM Symp. Reactor Dosimetry, EUR-6813 (1980).
4) Proc. 4th ASTM-EURATOM Symp. Reactor Dosimetry, NUREG/CP-0029 (1982).
5) Nakazawa M. and Sekiguchi A. : J. Atomic Energy Soc. Japan, **24**, 166 (1982).
6) Vlasov M.F., et al. : NUREG/CP-0004, 855 (1979).
7) Lederer C.M. and Shirley V.S. : "Table of Isotopes", 7th ed., John Wiley and Sons (1978).
8) Swann C.P. and Metzger F.R. : Phys. Rev., **100**, 1329 (1955).
9) Bornemisza P., Karolyi J. and Petö G. : Atmiki Közlemenyek, **10**, 112 (1968).
10) Temperley J.K. : Phys. Rev., **178**, 1904 (1969).
11) Hankla A.K., Fink R.W. and Hamilton J.H. : Nucl. Phys., **180**, 157 (1972).
12) Tourwé and Maene N. : EUR-6813, 1245 (1980).
13) Czock K.H., et al. : Int. J. Appl. Radiat. Isotop., **26**, 417 (1975).
14) Stantry D.C. and Butler J.P. : Can. J. Phys., **52**, 1421 (1974).
15) Pazsit A., et al. : Int. J. Appl. Radiat. Isotop., **26**, 621 (1975).
16) ENDF/B-V Dosimetry File, Tape No.531 and Material No.6436, evaluated by Schmittroth F. and Smith D.L. (1979).
17) Kobayashi K., et al. : J. Nucl. Energy, **27**, 741 (1973).
18) Yamamoto S., et al. : Annu. Rep. Res. Reactor Inst., Kyoto Univ., **11**, 121 (1978).
19) Robertson J.C., Audric B.N. and P. Kolkwski P. : J. Nucl. Energy, **27**, 139 (1973).
20) Gotoh H. and Yagi H. : Nucl. Instr. and Methods, **101**, 395 (1972).
21) Marion J.B. and Fowler J.L. : "Fast Neutron Physics", **2**, Interscience Pub., 2185 (1960).
22) Hopkins J. and Breit G. : Nucl. Data, **A9**, 145 (1971).
23) Gotoh H., to be published.
24) Cross W.G. and Ing H. : Nucl. Sci. Eng., **58**, 377 (1975).
25) Magurno B.A. : EUR-6813, 903 (1980).
26) Sakurai K. and Kondo I. : Nucl. Instr. and Methods, **187**, 649 (1981).
27) Seelmann-Eggebert W., Pfennig G. and Münzel H. : Nuklidkarte, (1974).
28) Sekiguchi A., et al. : NUREG/CP-0004, 1223 (1977).
29) Nakazawa M., et al. : UTNL-R-0099 (1981).
30) McElroy W.N., et al. : "A Computer-Automated Iterative Method for Neutron Flux Spectra Determination by Foil Activation", AFWL-TR-67-41 (1967).
31) Cullen D.E. : "Summary of ORR and YAYOI data for the REAL-80 Project Distributed 6 Feb. 1981", IAEA-NDS-33 (1981).

32) Engle W.W. : "A User's Manual for ANISN", K-1693 (1967).
33) Roy J.C. and Hawton J.J. : "Table of Estimated Cross Sections for (n,p), (n,α) and $(n,2n)$ Reactions in a Fission Neutron Spectrum", CRC-1003 (1960).
34) Catalogue of Reactor Experiments Inc. (1967).
35) Zijp W.L. and Baard J.H. : "Nuclear Data Guide for Reactor Neutron Metrology", ECN-70 (1979).
36) Iida H., et al. : JAERI-M 6205 (1975).
37) Hegedüs F. : "Détecteur de Fluence de Neutrons Rapides Base la Réaction $^{93}Nb(n,n')^{93m}Nb$", EIR-BERICHT NR-195 (1971).
38) Hegedüs F. : Reactor Radiation Metrology-Newsletter, **13**, 17 (1980).
39) Sakurai K. : Nucl. Instr. and Methods (in press).
40) Baht M.R. and Prince A. : "Evaluated Neutron Cross Sections", BNL-50383 (1973).